ELSEVIER

Journal of Fluids and Structures 19 (2004) 307–319

JOURNAL OF FLUIDS AND STRUCTURES

www.elsevier.nl/locate/jnlabr/yjfls

Characteristics of fin buffeting over delta wings

C. Lambert, I. Gursul*

Department of Mechanical Engineering, University of Bath, Bath BA2 7AY, UK

Received 24 July 2003; accepted 17 December 2003

Abstract

Characteristics of fin buffeting over various delta wings was investigated by measurements of fin tip acceleration, particle image velocimetry measurements, and flow visualization. For slender wings, there is a strong asymmetry with regard to the effect of fin location on the buffeting response, and largest response occurs for the inboard fin locations. For outboard fin locations, the buffeting is small, even at high angles of attack when vortex breakdown is well upstream. For inboard fin locations, the largest fin vibrations were found for breakdown locations well upstream of the fin, and when the shear layer of the breakdown region impinges on the fin. The results show that single-fin buffeting may be as important as twin-fin buffeting. For a wing with low sweep angle, vortex shedding rather than vortex breakdown may become the responsible mechanism, and large buffeting excitation for outboard fin locations at a specific incidence is possible. For a double-delta wing, the interaction of strake vortices with the wing flow has a major influence on the buffeting characteristics. Finally, it was found that a nonzero fin angle did not have much effect on the conclusions arrived in this study.

1. Introduction

Buffeting of lifting and nonlifting surfaces is a problem as typical fighter aircraft perform maneuvers at high angles of attack. Separated vortical flows originating from delta wings, leading-edge extensions and forebodies interact with wings, fins and tails. Vortex breakdown phenomenon is the most important source of buffeting over delta wings (Gursul, 1994), the most famous example of this is the F/A-18 fin buffeting. When the vertical tails are in the highly unsteady flow of vortex breakdown wake, large structural vibrations and severe structural fatigue damage may occur. Several investigators studied aspects of fin buffeting previously (Triplett, 1983; Lee and Brown, 1992; Washburn et al., 1993; Meyn and James, 1993; Lee and Tang, 1994; Bean and Wood, 1996; Moses and Ashley, 1998). Most of these studies were related to the characterization of the unsteady fin pressure due to the vortical flow, and buffeting response of the fin structure. A summary of previous investigations is given by Wolfe et al. (1995a) and Gursul and Xie (1999). It was reported that unsteady loading on the fin structure strongly depends on the location of fin with respect to the vortex, and the direct impingement (or ''head-on collision'' case) does not necessarily produce the largest unsteady forces (Wolfe et al., 1995b).

Detailed flow field studies were performed in several investigations that revealed the distortion of incident vortex, vortex splitting, and unsteady flow separation from the leading-edge of the fin (Mayori and Rockwell, 1994; Wolfe et al., 1995b; Canbazoglu et al., 1995; Gordnier and Visbal, 1996). The effect of aeroelastic deflections of fins on vortex breakdown and fin buffeting was considered in recent investigations (Gursul and Xie, 2001; Sahin et al., 2001). It was shown that the fin deflections may be important depending on the fin location with respect to the leading-edge vortex. Gursul and Xie (2001) showed that large sensitivity of vortex breakdown is only observed for particular fin locations.

*Corresponding author. Fax: +44-1225-386928.
E-mail address: ensiag@bath.ac.uk (I. Gursul).

0889-9746/$ - see front matter © 2004 Elsevier Ltd. All rights reserved.
doi:10.1016/j.jfluidstructs.2003.12.007

Hence, the relative position of fin with respect to the leading-edge vortex is important in determining the sensitivity of vortex breakdown to the fin oscillations.

Although leading-edge vortices are primary sources of fin buffeting, the effect of location of fin with respect to the vortices is not clearly understood. In a recent investigation (Lambert and Gursul, 2001), it was reported that buffeting response is not symmetric with respect to the fin location, i.e. inboard locations produce larger buffeting response. The first objective of this work is to investigate the characteristics of fin buffeting over delta wings in detail. The location of the fin was chosen as main variable, and fin-buffeting vibration measurements, particle image velocimetry measurements and flow visualization were carried out. It is also noted that there has been no systematic study of the effect of wing geometric parameters such as incidence and sweep angle on fin buffeting. In fact, not only the strength of the vortices, but also their structure varies as the sweep angle or incidence is changed. Slender wing vortices and vortex breakdown are replaced by vortex shedding at higher incidences and for low sweep angles, which can also cause buffeting (Gursul and Xie, 1999). The second objective of this work is to investigate characteristics of fin buffeting over various delta wing configurations, changing from very slender wings to low sweep wings.

2. Experimental setup

For the majority of the experiments reported here, a flexible fin was used to characterize the buffeting excitation. Most investigators used rigid fins in previous work, which eliminate structural resonance that occurs when the excitation frequency of the vortex flow coincides with the natural frequency of the fin. However, this approach requires the measurement of pressure fluctuations at many locations and integration over the fin surface. On the other hand, with a flexible fin, the buffet excitation can be obtained properly from measurements of the fin tip acceleration as long as the resonance condition is avoided. This approach is much more efficient than rigid fin experiments, and has been widely used in this work.

A flexible fin shown in Fig. 1(a) was designed and fabricated. It consists of a thin aluminum spar surrounded by several wood segments to provide aerodynamic shaping. The advantages that the wood sections offer are low material density and ease of fabrication. These sections were attached to the spar with small bolts. With this design, the contribution of the wood sections to the bending stiffness of the spar is small. The dimensions of the spar were chosen to obtain the natural frequencies of the first bending mode for a typical modern combat aircraft. The thickness of the spar was 2 mm. The leading edge of the fin was double bevelled at an angle of 30°. The main dimensions of the fin are given in Fig. 1(a) [also by Phillips et al., (2003)]. The spar was attached to the delta wing by a bracket near the trailing edge of the wing.

Experiments were carried out for this configuration in a 2.12 m × 1.51 m low-speed wind tunnel. The experimental setup, which uses half-model delta wings and a splitter plate, is shown in Fig. 1(b). It is noted that vortex-pair interactions may be important for twin fin configurations, and cannot be simulated with half-models. The splitter plate used was 800 mm in diameter and 6 mm thick, with rounded leading edge. This splitter plate was in turn attached to a central support strut and the inverted wing was then suspended in the center of the wind tunnel. Four delta wing models with sweep angles of $\Lambda = 75°$, 70°, 65°, 50°, and a double delta wing with 76°/40° sweep angles as shown in Fig. 1c were used in the experiments. The geometry of the double delta wing was the same as one used by several investigators previously (Ekaterinaris et al., 1995; Verhaagen, 1999). The chord length and thickness of all wings were of $c = 500$ mm and $t = 15$ mm, respectively. The lee surfaces were flat, whereas the leading-edges were bevelled at 45° on the windward side. The Reynolds number based on the chord length varied from $\mathrm{Re} = 3.5 \times 10^5$ to 1.1×10^6, although the majority of the experiments were conducted at $\mathrm{Re} = 1.07 \times 10^6$.

Although the majority of the wind tunnel experiments were conducted for the half-model wings, a full-model delta wing was also tested for $\Lambda = 75°$ only. For the full model, a sting was attached to the wing and an existing high-α test rig was used to support the model and sting. Details of the sting and support are given by Gray et al. (2003). The angle of attack can easily be adjusted from outside the tunnel, while a pantograph arrangement keeps the model in the center of the cross-section of the tunnel.

Buffeting response of the flexible fin was investigated by measuring fin vibration levels with a tip accelerometer. The location of the accelerometer is shown in Fig. 1(a). It is located at a vertical distance of 120 mm above the wing surface. The measurement uncertainty for the tip acceleration is estimated as 2%. In addition to the calculating the r.m.s. value of the wing tip acceleration, the spectra of the tip acceleration was examined for each case. The vibration frequency ($f \backsimeq 33$ Hz), which is the natural frequency of the first bending mode, is independent of free stream velocity (Lambert and Gursul, 2001). In addition, there is little influence of the angle of attack on the vibration frequency.

Flow visualization was performed using an Aerotech paraffin smoke generator. The wind tunnel was run at 3 m/s (this value was decided upon in order to maintain a Reynolds number of approximately 100 000 in order to avoid any

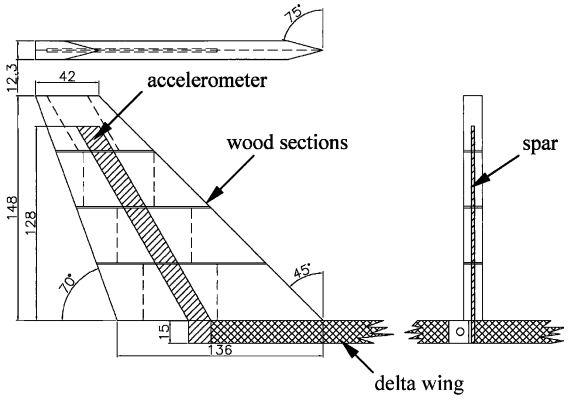

(a) Design of flexible fin

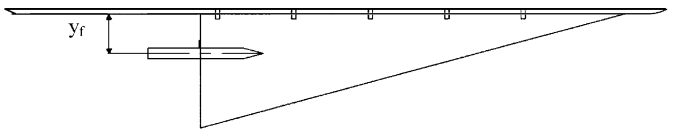

(b) Half delta wing model, fin and splitter plate

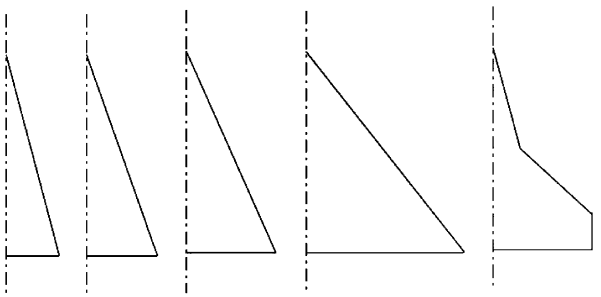

(c) Schematic drawings of all half model delta wing designs
($\Lambda = 75^0, 70^0, 65^0, 50^0, 76^0/40^0$)

Fig. 1. Overview of the experimental setup; (a) design of flexible fin, (b) half delta wing model, fin and splitter plate, (c) Schematic drawings of all half model delta wing designs ($\Lambda = 75°$, 70°, 65°, 50°, 76°/40°)

low Reynolds number effects). A Panasonic digital video camera was used to capture flow visualization images. At selected spanwise positions of the fin ($y_f/s = 0.2$, 0.4, 0.6, 0.8, and 1.0, where s is the local semispan of the wing at the leading edge of the fin), images were taken from the side of the tunnel and from underneath the wind tunnel for side and top views of the leading-edge vortex. The measurement uncertainty of vortex breakdown location was estimated to be 2–3% of the chord length, depending on incidence and smoke concentration. The mean (time-averaged) breakdown location was found by analysing flow visualization images for long time records (on the order of 10^3 convective time units).

Flow field measurements were carried out by a particle image velocimetry (PIV) system in a water tunnel located in the University of Bath. The water tunnel has a horizontal working section, with a cross-sectional area of 15 in × 20 in (381 mm × 508 mm). The full-model delta wing and fin were designed and scaled to those used in the wind tunnel experiments. The model was mounted upside down in the tunnel, and was supported with a vertical strut underneath the wing in order to minimize interference effects. The chord length is $c = 250$ mm, giving a Reynolds number around $\mathrm{Re} = 100\,000$ for $U_\infty = 40$ cm/s. At the maximum angle of attack $\alpha = 40°$, the blockage ratio was 6%. The PIV system utilized a pair of 30 mJ Nd:YAG lasers with a TSI PIVCAM 10–30 camera (operating at 30 frames/s, giving 15

measurements per second in cross-correlation). The software Insight was used to post-process the data. The flow was seeded with Polyamid particles of mean diameter of 50 μm and a density of 1.03 g/cm^3, making them slightly less than neutrally buoyant. The laser sheet was placed at the trailing edge, and normal to the free stream velocity, and the cross-flow velocity field was measured by illuminating the plane from below. The cross-flow plane was viewed by the camera placed near the downstream viewing window of the tunnel.

3. Results

Since previous results (Lambert and Gursul, 2001) indicated a strong sensitivity to the fin location y_f/s, the tip acceleration was measured as a function of fin location and the free stream velocity U_∞. The variation of root-mean-square value of acceleration as a function of free stream velocity for different values of angle of attack is shown in Fig. 2 for $y_f/s = 0.4$ and 0.6, for $\Lambda = 75^\circ$. Detailed results for other values of y_f/s with increments of 0.1 are given by Lambert and Gursul (2001). Generally speaking, the r.m.s acceleration increases with increasing free stream velocity for a given fin location. Local maximums are observed around certain U_∞ (particularly at low speeds) and at high angle of attack due to the structural resonances. The variation of the tip acceleration is more sensitive to the changes in angle of attack. Sudden increases are observed at high angle of attack, whereas there is little change at low angles of attack. The sudden increase of buffeting when the incidence is increased from 25° to 30° in Fig. 2(a) is due to the vortex breakdown moving upstream of the fin.

A more appropriate form of presenting the data is the variation of dimensionless acceleration parameter, which includes the effect of the free stream velocity. If the r.m.s. acceleration $a_{\text{r.m.s.}}$, free stream velocity U_∞, and the spar

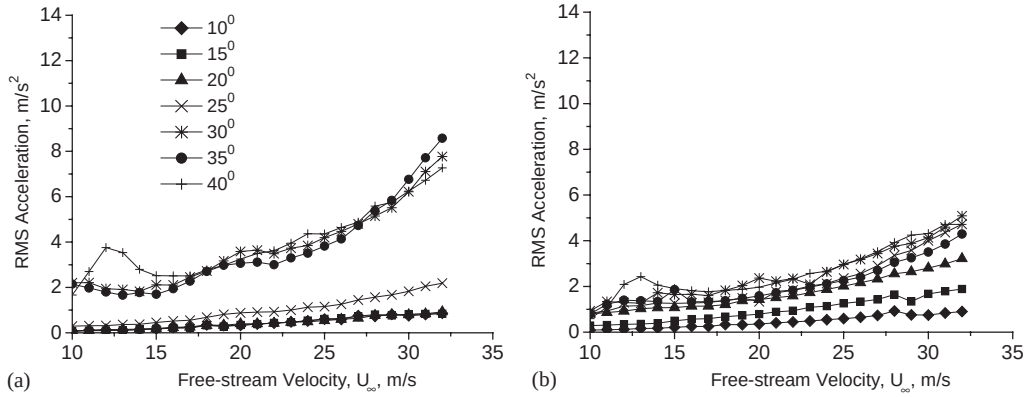

Fig. 2. Variation of the root-mean-square value of fin tip acceleration as a function of free stream velocity for $\Lambda = 75^\circ$ and (a) $y_f/s = 0.4$ and (b) $y_f/s = 0.6$.

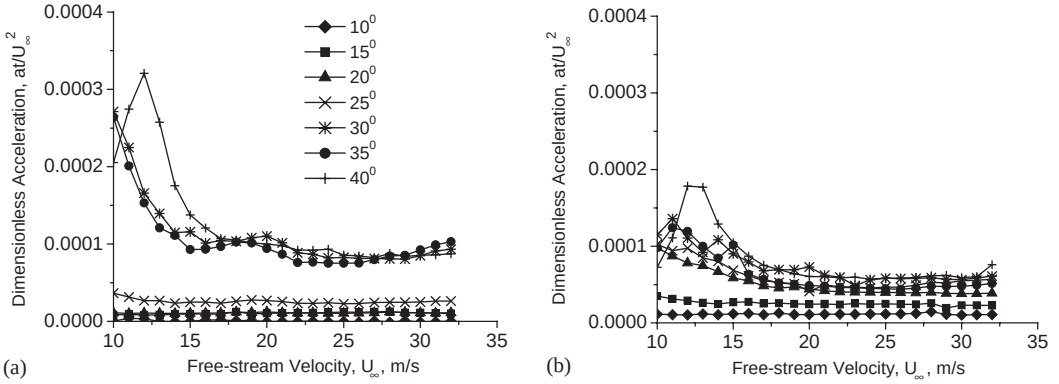

Fig. 3. Variation of dimensionless tip acceleration as a function of free stream velocity for $\Lambda = 75^\circ$ and (a) $y_f/s = 0.4$ and (b) $y_f/s = 0.6$.

thickness t are considered as main variables, a dimensionless number $a_{\text{r.m.s.}}\, t/U_\infty^2$ can be formed. A similar approach was used by Mabey (1973) in presenting the tip acceleration data. The variation of dimensionless acceleration as a function of free stream velocity (corresponding to the data shown in Fig. 2), is shown in Fig. 3. It can be seen that the dimensionless acceleration is constant for low and moderate angles of attack over the free stream velocity range tested, but for higher angles of attack, there is a local maximum near the low speed end. This indicates fin structural resonance with the helical mode instability of vortex breakdown. For example, for $y_f/s = 0.4$ and $\alpha = 40^\circ$, the local maximum occurs at $U_\infty = 12$ m/s, which corresponds to a dimensionless frequency of $fc/U_\infty = 1.37$ (where the f is the frequency of the fin vibrations). This value compares reasonably well with the measurements of the helical mode instability (Gursul, 1994) over delta wings, which revealed that fc/U_∞ is around 1.20 at $\alpha = 40^\circ$. For $U_\infty \geqslant 15$ m/s, the dimensionless acceleration is approximately constant even at higher angles of attack, and hence the structural resonance is absent. This was also confirmed for other fin locations by Lambert and Gursul (2001). For other wings, similar results are expected as the dominant frequency of the helical mode instability (Gursul, 1994) remains in the same range for various delta wings. Indeed, it was confirmed by Lambert (2003) that the structural resonance is absent for $U_\infty \geqslant 15$ m/s for all models at various incidences. Hence, the r.m.s. tip acceleration is a direct measure of buffet excitation in the resonance-free conditions.

In order to avoid the resonance conditions and hence obtain a meaningful comparison for the effect of fin location, the r.m.s. tip acceleration is shown in Fig. 4 for the free stream velocity $U_\infty = 30$ m/s, which is far away from the structural resonance conditions. For the rest of this paper, all tip acceleration data will refer to $U_\infty = 30$ m/s. In Fig. 4, it is seen that the buffeting response is very small for the most outboard fin location ($y_f/s = 1.0$) for all angles of attack. The maximum buffeting response occurs near the vortex axis ($y_v/s \approx 0.60$) for low angles of attack, although this is a very broad peak. The spanwise location of the vortex was estimated from the pressure measurements across the span at $x/c = 0.5$ in the absence of the fin (Lambert and Gursul, 2001). The location of the pressure (suction) peak is only slightly affected by the angle of attack, showing that the spanwise location of the leading edge vortex is roughly constant. As the angle of attack is increased, the local maximum with very well-defined peaks shifts to inboard locations. However, as noted above, the spanwise location of the vortex axis does not change much with angle of attack. Hence, the shift in the location of the maximum buffeting response is due to the direct impingement of the shear layer in the breakdown region onto the fin. Here, the shear layer refers to the region of large velocity gradient formed between nearly stagnant flow near the center of vortex and the free stream.

In order to understand this interaction better, flow visualization was performed. Fig. 5 shows flow visualization pictures as a function of fin location y_f/s for $\alpha = 30^\circ$. Variation of the time-averaged breakdown location as a function of fin location at different angles of attack is shown in Fig. 6. It is noted that the instantaneous breakdown locations seen in pictures in Fig. 5 are somewhat different than the time-averaged breakdown locations in Fig. 6. Typical fluctuations of breakdown location can be large, varying from $(x_{bd})_{\text{r.m.s.}}/c \approx 0.03$ for slender wings to $(x_{bd})_{\text{r.m.s.}}/c \approx 0.06$ for nonslender wings. The mean breakdown location is roughly the same for all fin locations. For $y_f/s = 0.2$ shown in Fig. 5, the vortex breakdown region does not impinge on the fin, and the resulting fin buffeting response is small (see Fig. 4). However, note that $y_f/s = 0.4$ produces the largest buffeting response, as the fin is affected by the impinging shear layer. With further outboard displacement of the fin location towards the leading edge, the buffeting response becomes very small. It is interesting that inboard fin locations can cause larger buffeting response than outboard locations. The physical mechanism behind this asymmetric response (with respect to the vortex axis) is not clear. Comparison of Fig. 6

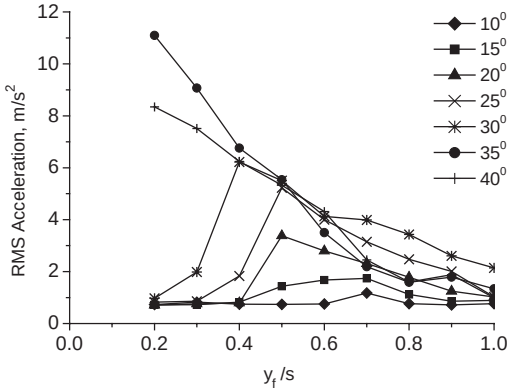

Fig. 4. Variation of r.m.s. acceleration as a function of fin location for $\Lambda = 75^\circ$, $U_\infty = 30$ m/s.

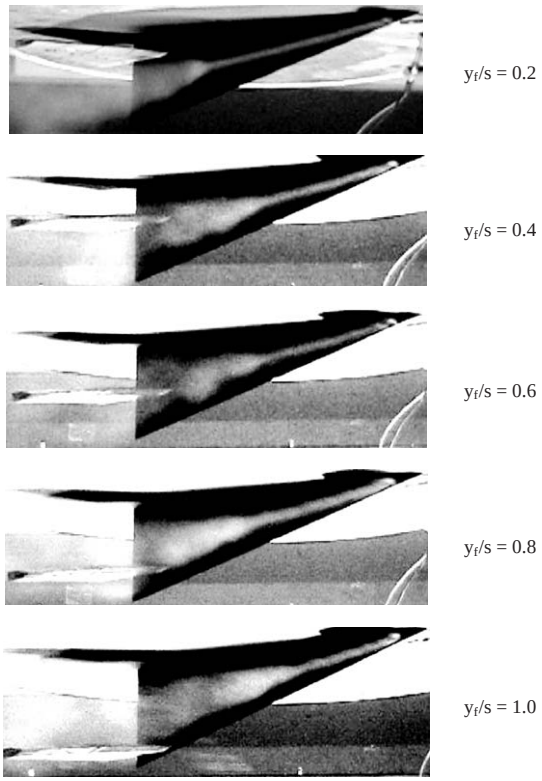

Fig. 5. Flow visualization for different values of fin location for $\Lambda = 75^\circ$ and $\alpha = 30^\circ$.

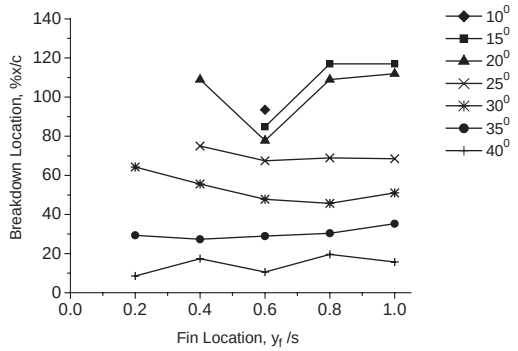

Fig. 6. Variation of the vortex breakdown location as a function of fin location at different angles of attack for $\Lambda = 75^\circ$.

with the tip acceleration shown in Fig. 4 amplifies the importance of fin position even when breakdown location is nearly the same for high angle of attack. Hence there is an apparent asymmetry with regard to the effect of fin location on the buffeting response.

Note that the largest buffeting response occurs for the most inboard fin locations ($y_f/s = 0.2$ and 0.3) at the highest angles of attack ($\alpha = 35^\circ$–40°). In particular, for $y_f/s = 0.2$, there is very little buffeting at low to moderate angles of attack (up to $\alpha = 30^\circ$), but there is a very sharp increase in buffeting at $\alpha = 35^\circ$ and 40°. Corresponding flow visualization pictures are shown in Fig. 7. The picture for $\alpha = 35^\circ$ indicates that the shear layer of the breakdown region impinges onto the fin. These results also imply that single-fin buffeting may be as important as twin-fin buffeting. Further evidence for this conclusion will be presented later on in the paper. The location of vortex breakdown and the relative position of the shear layer with respect to the fin, as well as the variation of the strength of the vortices as the

(a)

(b)

Fig. 7. Flow visualization for (a) $\alpha = 30^\circ$ and (b) $\alpha = 35^\circ$ for $\Lambda = 75^\circ$ and $y_f/s = 0.2$.

angle of attack varies are likely be important factors. Returning to the discussion of Fig. 4, an interesting case is for $y_f/s = 0.6$ (direct impingement or "head-on collision") for which vortex breakdown is always upstream of the fin. In this case, the fin buffeting response first increases with angle of attack, and then remains nearly constant at high angle of attack. For fin locations $y_f/s = 0.8$ and 1.0, it is seen that the buffeting response actually decreases at high angle of attack.

In order to understand why inboard locations produce much higher buffeting response, the unsteady flow field downstream of vortex breakdown needs to be considered. To understand the interaction of unsteady wake with the fin, PIV measurements were carried out over a full model in the water tunnel. In Fig. 8, the results of the PIV measurements in the cross-flow plane at the trailing edge are shown for $y_f/s = 0.2$ and $\alpha = 35^\circ$. The constant contours of the time-averaged cross-flow velocity V/U_∞ (Fig. 8a), also combined with velocity vectors (Fig. 8b), normalized vorticity $\omega s/U_\infty$ (Fig. 8c), and normalized r.m.s. cross-flow velocity $v_{\text{r.m.s.}}/U_\infty$ (Fig. 8d) are shown. The location of vortex breakdown is far upstream ($x_{bd}/c \approx 0.3$), and hence the breakdown wake at the trailing edge is very large. The size of the nearly swirl free region centered around the vortex axis is on the order of the semispan. The shear layer that borders the vortex core is very close to the fin, and interacts with it. Note that the largest fin buffeting level was observed in the wind tunnel experiments for this configuration. At this location far downstream from the vortex breakdown, the vorticity and r.m.s. velocity magnitude are fairly uniform over the core, although there is some evidence of ring-like structure. This is consistent with the available data in the literature, which indicate that the r.m.s. value of the velocity fluctuations downstream of vortex breakdown is fairly axisymmetric, and therefore cannot explain the observed asymmetric buffeting response (Kommallein and Hummel, 1993; McCormick and Gursul, 1996; Mitchell et al., 2000). Note that the time-averaged cross-flow velocity is always higher inboard of the vortex core, which is suspected to play an important role in the observed asymmetry for the buffeting response. If it is assumed that the flow may be regarded as quasi-steady, it can be shown (Davenport, 1977) that the fluctuating pressure will be proportional to $\rho U q'$, where U and q' denote time-averaged and fluctuating velocity. Although all three components of velocity is not measured in this work, the cross-flow velocity suggests that asymmetry in the time-averaged velocity might be responsible for the observed asymmetry for the buffeting response.

In Fig. 9, the results of the PIV measurements in the cross-flow plane at the trailing edge are shown for $y_f/s = 0.6$, which is the case of "head-on collision". The time-averaged velocity contours show that the vortex core region is split by the fin, and is less axisymmetric. The tip of the fin is further away from the shear layer. Again, larger cross-flow velocity is observed inboard of the vortex core, although the fin itself remains in a relatively swirl free zone. Comparing Figs. 8 and 9, and fin buffeting response discussed earlier, it is concluded that the largest buffet excitation is generated when the shear layer closely interacts with the fin.

In order to study the effect of wing sweep angle, fin tip acceleration was measured for all wings shown in Fig. 1(c). The results for the three slender wings ($\Lambda = 75^\circ$, 70°, 65°) are shown in Figs. 10–12 as a function of $2y_f/b$, where b is the span. It is seen that the trend is the same, i.e. inboard locations produce larger buffeting for all three slender wings. However, the variation of the maximum buffeting with spanwise location becomes more gradual with decreasing sweep angle. Other features are very similar for all wings (for example, the shifting of the peaks inboard with increasing angle of attack is observed for all three wings). One noticeable difference for the least slender wing ($\Lambda = 65^\circ$) is that at the highest incidence of $\alpha = 40^\circ$, the buffeting level is nearly constant for all fin locations. At this incidence, stalled flow over the wing is dominant rather than any organized vortical flow.

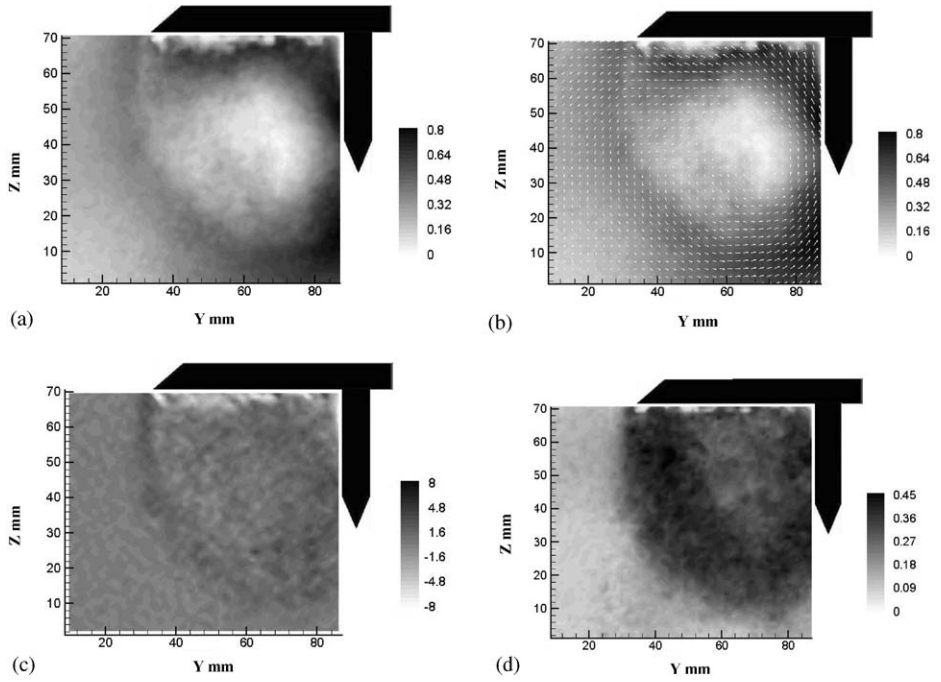

Fig. 8. PIV results from water tunnel experiments for $y_f/s = 0.2$: (a) contours of mean velocity; (b) contours and vectors of mean velocity; (c) vorticity; (d) r.m.s. velocity.

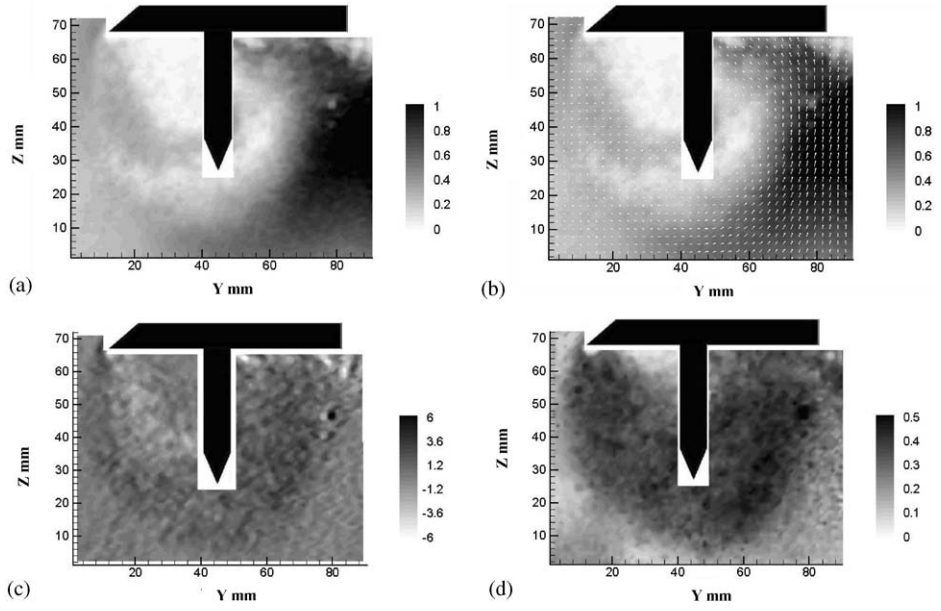

Fig. 9. PIV results from water tunnel experiments for $y_f/s = 0.6$: (a) contours of mean velocity; (b) contours and vectors of mean velocity; (c) vorticity; (d) r.m.s. velocity.

In order to study the fin buffeting over a nonslender wing, a wing with relatively low sweep angle was considered. The variation of the r.m.s. tip acceleration for $\Lambda = 50^\circ$ wing is shown in Fig. 13(a). For low angles of attack $\alpha = 10$–20°, similar trends as slender wings are observed. However, for larger angles of attack, the response of the flexible fin is very different. For $\alpha \geqslant 30^\circ$, the r.m.s. tip acceleration is roughly constant. As the formation of leading edge vortices and

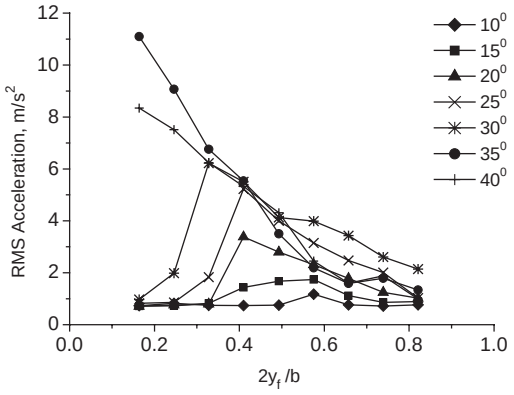

Fig. 10. Variation of r.m.s. acceleration as a function of fin location, $2y_f/b$, for $\Lambda = 75°$.

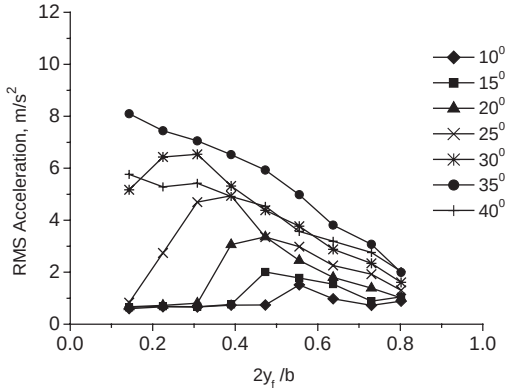

Fig. 11. Variation of r.m.s. acceleration as a function of fin location for $\Lambda = 70°$.

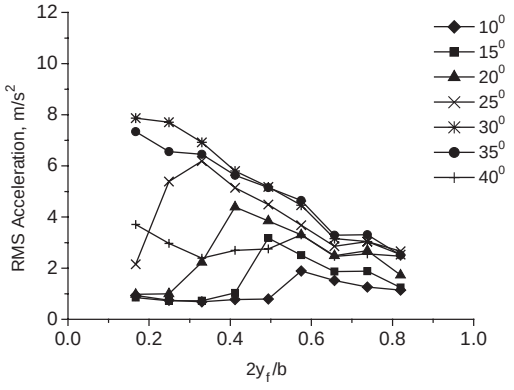

Fig. 12. Variation of r.m.s. acceleration as a function of fin location for $\Lambda = 65°$.

vortex breakdown are confined to lower incidences ($\alpha < 20°$), vortex shedding rather than stable leading-edge vortices is the dominant flow mechanism at higher incidences. For $\alpha = 25°$, relatively large buffeting excitation is observed for outboard fin locations, showing a local maximum around $2y_f/b = 0.77$. For this particular fin location, flow visualization pictures for $\alpha = 15°$ and $25°$ are shown in Fig. 13(b). For $\alpha = 25°$, the separated shear layer seems to be impinging upon the fin, showing that fin buffeting can be induced by mechanisms other than vortex breakdown. For larger incidences, the fin appears to be missing the separated shear layer, resulting in substantially smaller fin vibrations.

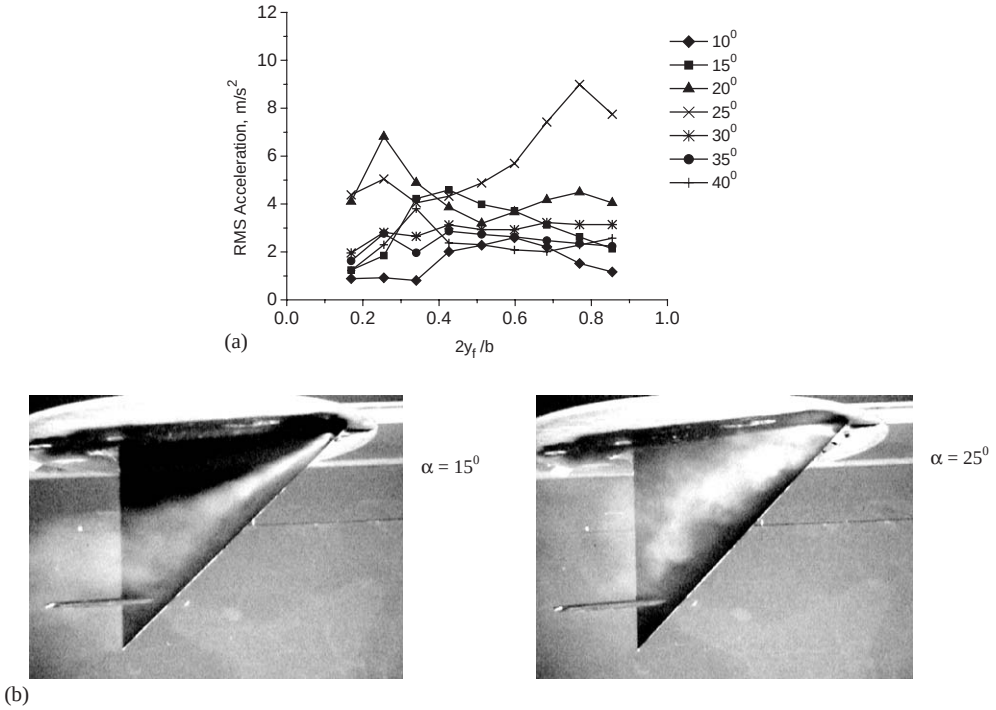

Fig. 13. (a) Variation of r.m.s. acceleration as a function of fin location for $\Lambda = 50^\circ$; (b) Flow visualisation pictures for $\Lambda = 50^\circ$ and $2y_f/b = 0.77$.

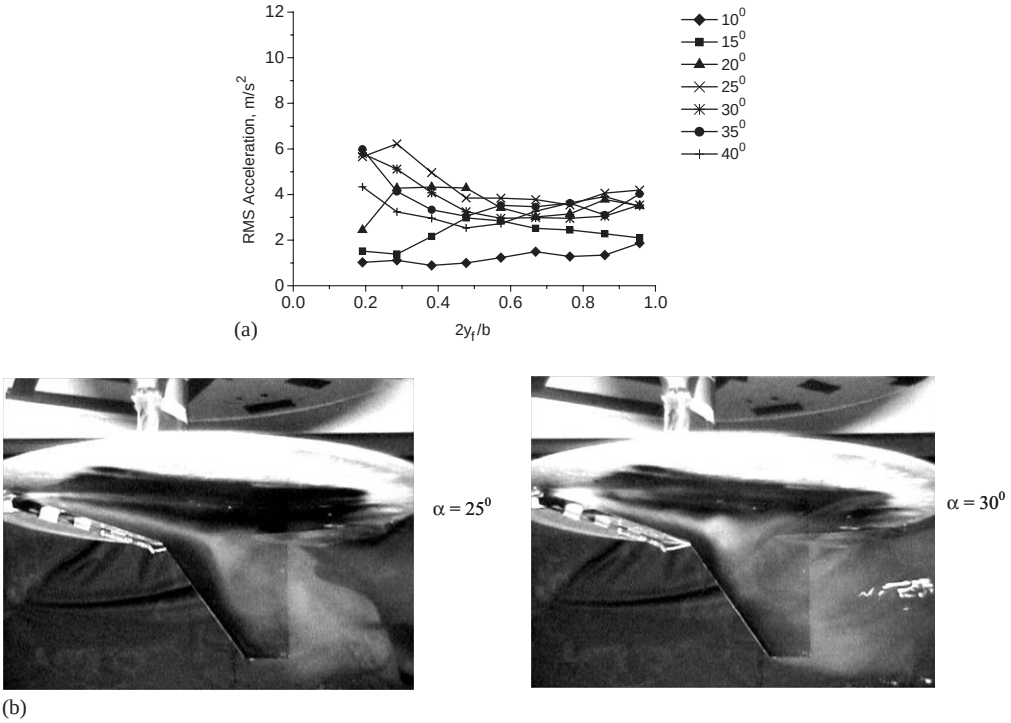

Fig. 14. (a)Variation of r.m.s. acceleration as a function of fin location for $\Lambda = 76^\circ/40^\circ$; (b) Flow visualisation pictures for $\Lambda = 76^\circ/40^\circ$ and $2y_f/b = 0.19$.

The double delta wing model shown in Fig. 1(c) is more representative of an aircraft, and therefore is an interesting case with regard to the fin buffeting. Fig. 14(a) shows the variation of the r.m.s. tip acceleration as a function of spanwise fin location at different angles of attack. The inboard locations produce slightly larger buffeting, but overall the buffeting excitation is small and does not depend on the fin location significantly. Although the 76°/40° wing has a highly slender strake, the wing with such low sweep angle has a major influence on the strake vortices. The wing vortices are stronger than the strake vortices, hence they breakdown first. The breakdown of the strake vortices is then triggered by the breakdown of the wing vortices (Verhaagen, 1995). Although the breakdown of the strake vortices over the wing can be observed at large incidences as shown in Fig. 14(b) for $\alpha = 25°$ and 30°, the wing vortices disappear and stalled flow dominates over the wing. The breakdown region and resulting stagnant flow region appear to be very large compared to that of slender vortices. This is due to stalled wing flow and gives rise to nearly same level of buffeting for

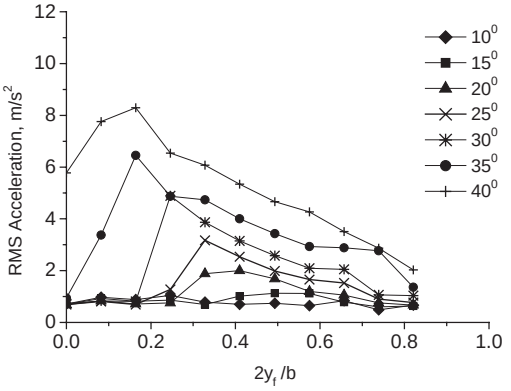

Fig. 15. Variation of r.m.s. acceleration as a function of fin location for the full delta wing model, $\Lambda = 75°$.

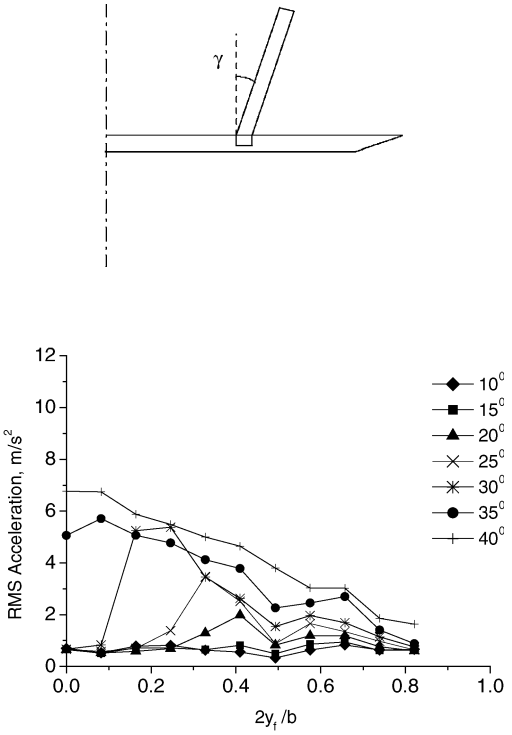

Fig. 16. Variation of r.m.s. acceleration as a function of fin location for the full delta wing model with fin at $\gamma = 25°$.

different fin locations. Even at high angles of attack when the vortex breakdown location is far upstream of the fin, tip acceleration results are very different than those of slender wings. It is believed this is due to the totally separated flow over the wing in which the fin is immersed.

Some experiments were conducted with a full-model wing with $\Lambda = 75^\circ$ in order to understand single-fin buffeting (fin located at wing center-line) and also to see effects of the half-model/splitter plate arrangement on the results. The variation of the r.m.s. tip acceleration is shown in Fig. 15 as a function of fin location. It is seen that fin vibration level can be very large at high incidence ($\alpha = 40^\circ$) when the fin is located at the wing center-line. The overall variation of r.m.s. acceleration is similar to that of half-model shown in Fig. 10. There are some differences in measured vibration levels, in particular for inboard fin locations and high incidence ($\alpha = 35^\circ$ and 40°). This may be due to the presence of the splitter plate, the effects of boundary layer formation over the splitter plate and its influence on the leading-edge vortex. Nevertheless, the results confirm that inboard fin locations produce larger buffeting, and single-fin buffeting ($y_f = 0$) may be important at high incidence.

Finally, it is noted that fins/tails are placed with an angle in many aircraft configurations. In order to see if this has any effect on the conclusions arrived in this study, some exploratory experiments were conducted. In Fig. 16, the variation of r.m.s. tip acceleration is shown as a function of fin location for the full-model $\Lambda = 75^\circ$ wing and fin angle of 25° (the definition of the fin angle is given in the inset schematically). It is seen that the results are very similar and confirms earlier conclusions. Inboard fin locations (even at the wing center-line) and high incidence together give rise to large fin buffeting excitation.

4. Conclusions

In this investigation, characteristics of fin buffeting over various delta wings was investigated by measurements of fin tip acceleration, particle image velocimetry measurements, and flow visualization. For slender wings, there is a strong asymmetry with regard to the effect of fin location on the buffeting response, and largest response occurs for the inboard fin locations. For outboard fin locations, the buffeting is small, even at high angles of attack when vortex breakdown is well upstream. Maximum buffeting response occurs when the fin is located near the vortex axis for low angles of attack, but the location of the maximum buffeting shifts to inboard locations as the angle of attack is increased. For inboard fin locations, the largest fin vibrations were found for breakdown locations well upstream of the fin, and when the shear layer of the breakdown region impinges on the fin. The results show that single-fin buffeting may be as important as twin-fin buffeting. Particle image velocimetry measurements for an inboard fin location confirmed that the shear layer that borders the vortex core closely interacts with the fin.

Although inboard fin locations produce larger buffeting for all slender delta wings, the variation of the maximum buffeting excitation with spanwise location of the fin becomes more gradual with decreasing sweep angle. On the other hand, fin buffeting characteristics are very different for a wing with low sweep angle. Vortex shedding rather than vortex breakdown may become the mechanism responsible and large buffeting excitation for outboard fin locations at a specific incidence is possible. For a double-delta wing, the interaction of strake vortices with the wing flow has a major influence on the buffeting characteristics, and results in roughly the same level of buffeting for different fin locations. Finally, it was found that a nonzero fin angle did not have much effect on the conclusions arrived in this study.

Acknowledgements

This work was sponsored by the European Office of Aerospace Research and Development, Air Force Office of Scientific Research, USAF, under Contract No. F61775-00-WE025.

References

Bean, D.E., Wood, N.J., 1996. Experimental investigation of twin-fin buffeting and suppression. Journal of Aircraft 33, 761–767.

Canbazoglu, S., Lin, J.C., Wolfe, S., Rockwell, D., 1995. Buffeting of fins: distortion of incident vortex. AIAA Journal 33, 2144–2150.

Davenport, A.B., 1977. The prediction of the response of structures to gusty wind, International Research Seminar on Safety of Structures under Dynamic Loading. Norwegian Institute of Technology.

Ekaterinaris, J.A., Coutley, R.L., Schiff, L.B., Platzer, M.F., 1995. Numerical investigation of high incidence flow over a double-delta wing. Journal of Aircraft 32, 457–463.

Gordnier, R.E., Visbal, M.R., 1996. Numerical simulation of the impingement of a streamwise vortex on a plate. International Journal of Computational Fluid Dynamics 12, 49–66.

Gray, J.M., Gursul, I., Butler, R., 2003. Aeroelastic response of a flexible delta wing due to unsteady vortex flows. AIAA-2003-1106, 41st Aerospace Sciences Meeting and Exhibit, Reno, NV, USA.

Gursul, I., 1994. Unsteady flow phenomena over delta wings at high angle of attack. AIAA Journal 32, 225–231.

Gursul, I., Xie, W., 1999. Buffeting flows over delta wings. AIAA Journal 37, 58–65.

Gursul, I., Xie, W., 2001. Interaction of vortex breakdown with an oscillating fin. AIAA Journal 39, 438–446.

Kommallein, S., Hummel, D., 1993. In: Gersten, K., (Ed.), LDA Investigations of the Separated Flow Over Slender Wings, Physics of Separated Flows—Numerical, Experimental, and Theoretical Aspects. Vieweg, Braunschweig, pp. 275–282.

Lambert, C., 2003, Fin buffeting over delta wings. Ph.D. Thesis, Department of Mechanical Engineering, University of Bath, UK.

Lambert, C., Gursul, I., 2001. Buffeting of a flexible fin over a delta wing. AIAA 2001-2426, 19th AIAA Applied Aerodynamics Conference, 11–14 June, Anaheim, California, USA.

Lee, B.H.K., Brown, D., 1992. Wind-tunnel studies of F/A-18 tail buffet. Journal of Aircraft 24, 146–152.

Lee, B.H.K., Tang, F.C., 1994. Characteristics of the surface pressures on a F/A-18 vertical fin due to buffet. Journal of Aircraft 31, 228–235.

Mabey, D.G., 1973. Beyond the buffet boundary. Aeronautical Journal 77, 201–215.

Mayori, A., Rockwell, D., 1994. Interaction of a streamwise vortex with a thin plate: a source of turbulent buffeting. AIAA Journal 32, 2022–2029.

McCormick, S., Gursul, I., 1996. Effect of shear layer control on leading edge vortices. Journal of Aircraft 33, 1087–1093.

Meyn, L.A., James, K.D., 1993. Full scale wind tunnel studies of F/A-18 tail buffet. AIAA-93-3519, AIAA Applied Aerodynamics Conference, Monterey, CA.

Mitchell, A.M., Molton, P., Barberis, D., Delery, J., 2000. Characterization of vortex breakdown by flow field and surface measurements. AIAA-2000-0788.

Moses, R.W., Ashley, H., 1998. Spatial characteristics of the unsteady differential pressures on 16% F/A-18 vertical tails. AIAA 98-0519, 36th Aerospace Sciences Meeting and Exhibit, January 12–15, Reno, NV, USA.

Phillips, S., Lambert, C., Gursul, I., 2003. Effect of a trailing-edge jet on fin buffeting. Journal of Aircraft 40, 590–599.

Sahin, B., Akilli, H., Lin, J.C., Rockwell, D., 2001. Vortex breakdown-edge interaction: consequence of edge oscillations. AIAA Journal 39, 865–876.

Triplett, W.E., 1983. Pressure measurements on twin vertical tails in buffeting flow. Journal of Aircraft 20, 920–925.

Verhaagen, N.G., 1995. A study of the vortex flow over a 76/40-deg double-delta wing. AIAA Paper 95-0650.

Verhaagen, N.G., 1999. Effects of Reynolds number on the flow over 76/40 deg double-delta wings. AIAA 99-3117, 17th AIAA Applied Aerodynamics Conference, June 28–July 1, Norfolk, VA, USA.

Washburn, A.E., Jenkins, L.N., Ferman, M.A., 1993. Experimental investigation of vortex-fin interaction. AIAA 93-0050, 31st Aerospace Sciences Meeting and Exhibit, January 11–14, Reno, NV, USA.

Wolfe, S., Canbazoglu, S., Lin, J.C., Rockwell, D., 1995a. Buffeting of fins: an assessment of surface pressure loading. AIAA Journal 33, 223–2234.

Wolfe, S., Lin, J.C., Rockwell, D., 1995b. Buffeting at the leading-edge of a flat plate due to a streamwise vortex: flow structure and surface pressure loading. Journal of Fluids and Structures 9, 359–370.